PHILOSOPHICAL TRANSACTIONS A

Phil. Trans. R. Soc. A.

doi:10.1098/not yet assigned

Graphene production by cracking

Sivasambu Bohm[1*], Avinash Ingle[2], H. L. Mallika Bohm[1], Benji Fenech-Salerno[1], Shuwei Wu[1], Felice Torrisi[1]

[1]*Department of Chemistry, Molecular Sciences Research Hub, Imperial College London, White City Campus, Wood Lane, London W12 0BZ, UK,*

[2]*Centre Inter-universitaire de Recherche et d'Ingénierie des Matériaux - UMR CNRS 5085, France*

Keywords: Graphene, Graphene production, Graphene Oxide, 2D Materials, Transistors, Energy storage

Summary

In recent years, graphene has found its use in numerous industrial applications due to its unique properties. While its impermeable and conductive nature can replace currently used anticorrosive toxic pigments in coating systems, due to its large strength to weight ratio, graphene can be an important component as a next-generation additive for automotive, aerospace & construction applications. The current bottlenecks in using graphene & graphene oxide and other 2D materials are the availability of cost-effective, high-quality materials and their effective incorporation (functionalisation and dispersion) into the product matrices.

On overcoming these factors, graphene may attract significant demands in terms of volume consumption. Graphene can be produced on industrial scales and cost-effective top-down routes such as chemical, electrochemical, and/or high-pressure mechanical exfoliation. Graphene depending on end applications can be chemically tuned and modified via functionalisation so that easy incorporation into product matrices is possible. This paper discusses different production methods and their impact on the quality of graphene produced in terms of energy input. Graphene with an average thickness below five layers were produced by both methods with varied defects. However, a higher yield of graphene with a lower number of layers was produced by the high-pressure exfoliation route.

Main Text

1. Introduction

Ever since it was separated from bulk graphite for the first time in 2004 (1), graphene has come under the spotlight of scientific research. Graphene is defined as a single-atom flat monolayer made of sp^2-hybridized "honeycomb" carbon lattice (1–3). During the past two decades, scientists have discovered numerous unique properties of graphene such as high optical performance (4), high charge carriers mobility (due to electric field effect) (5) and thermal conductivity(6) and demonstrated a significant number of potential applications for this

*Author for correspondence (s.bohm@imperial.ac.uk). https://orcid.org/0000-0003-4559-882X

†Present address: Department of Chemistry, Molecular Sciences Research Hub, Imperial College London, White City Campus, 80 Wood Lane, London W12 0BZ, UK

material in its “gold rush” years (2,7), covering different areas including field emission (8,9), gas and biosensors (10,11), field-effect transistors (5), transparent electrodes (4,12), coatings (13), batteries (14,15) and printed electronics (16)(17). However, the progress of the devices mentioned above relies upon large-scale industrial production of graphene, which remains a major challenge (12). Thus, it has become an urgent task for researchers to develop a high-yield and low-cost mass production methods for graphene.

1.1. Production Methods of Graphene

In general, the synthesis methods consist of two main categories (18): bottom-up (synthesizing graphene atom by atom on a substrate) and top-down (separating already-existed graphene from its host material) method. Specifically, there are two major bottom-up methods; chemical vapour deposition (CVD) and epitaxial growth on the insulating substrate, both of which can synthesize high-quality graphene (12,18–21). Nevertheless, process conditions, such as high temperature, limit material choice and increase production cost (20,21). As a result, great efforts have been made to control the temperature to a lower level for CVD (20). On the other hand, top-down methods revolve around the idea of graphite exfoliation (22).

1.2. Top-Down methods

One of the most classic categories of this approach is the physical exfoliation (PE) of graphite, which includes the Nobel-prize-winning “scotch-tape” exfoliation experiment (1). While this groundbreaking research demonstrated the world’s first 2D material, it also inspired researchers to look into the potential of mechanically exfoliating 2D materials in the solid-state (23), such as micromechanical cleavage (24,25) and ball milling (22,26). These methods, however, fail to provide a sufficient yield and satisfactory flake sizes of graphene while remaining defect free (27). An alternative way to PE is to conduct it in a liquid phase, consisting of the dispersion of graphite in a solvent (aqueous or organic), exfoliation and purification (28); e.g., sonication and shear mixing exfoliation. In a typical liquid-phase PE process, graphite is broken into small fragments or few-layered flakes by a normal or shear force (23) (figure 1a). During the sonication process, cavitation is induced in the dispersion of graphite, and the solvent media then creates bubbles initiating the exfoliation process. Still, when more bubbles are formed on the lateral side, the shear force controls the separation process (23). By contrast, the shear force is dominant in shear mixing exfoliation and microfluidic exfoliation(29). Both of these techniques have proved to be potential candidates for scalable production, while efforts are still being made to reduce the intrinsically-induced defects (23,30) and to maintain larger flake sizes (29). Figure 2 shows three layers of graphene, weakly bonded by van der Waal forces.

Earlier studies focused on the chemical exfoliation (CE) of graphite (1,2), but they failed to produce a graphene-like 2D material (1). In chemical exfoliation, the graphite is treated with strong acid to introduce an oxygen-containing group on the surface resulting in graphite oxide (GO), facilitating the exfoliation process (31,32). After dispersed in a solvent, GO is thermally or chemically reduced to regain the conductivity (28,31). Unavoidably, this method will leave a significant number of defects and oxygen-containing group in the as-obtained graphite flakes.

Due to their considerable merits, electrochemical exfoliation (1) approaches have been extensively studied during the last few years. For example, they are less time-consuming, simpler to carry out, and can be operated in mild, less demanding process conditions (33). Therefore, these approaches have attracted both industrial and scientific attention. A typical EE system consists of three major elements: the electrolyte, the electrodes(usual graphite as the anode) and a voltage applied to the electrodes (33). The exfoliation is triggered when the anionic species in the electrolyte with oxygen radical is driven to intercalate the graphite flakes by the applied voltage and form graphite intercalation compounds (GICs), expanding the interlayers spacing (32) (figure 3a); the mechanism can be described by three-steps "intercalation-expansion-exfoliation" process; OH^- created by water reduction attacks the edge sites, expands the graphite layers and allows sulfate ions to intercalate; then the reduction of sulfate ions releases gas to further separate layers apart. Figure 3b demonstrates a typical EE process using sulfate salts solution as electrolyte (34).

The major challenges for graphene commercialization have remained as the yield and quality. As a result, exfoliation methods and related process parameters are urgently required to be further optimized to achieve a low-cost and scalable production.

1.3 Factors affecting Graphene Quality

In a broader sense, cracking in solid materials is seen as a process that imparts a negative impact on material properties. However, understanding how the mechanism and energy transition of relevant cracking processes that affect layered materials is paramount to achieving reduced energy usage, optimum product yield and process efficiency for successful commercial 2D materials production. This is because the highest cost contribution of the top-down routes comes from energy usage.

1.3.1 Energy Input

The internal energy of the system in the context of exfoliation is dominated by the interlayer interaction, and it is suggested that theoretically, the exfoliation energy is defined as the energy required to peel off a single layer from the surface of the bulk materials or to separate all the layers of the bulk and divided by the number of layers. One research group (35) has simplified this statement and subsequent computation load by re-defining the energy equation as "*the exfoliation energy is equal to the difference between the ground-state energy of the bulk per layer and that of an isolated layer*". Assuming only van der Waals interactions between layers, the team has deduced the exfoliation energy for several materials (i.e., graphene, h-BN, etc.). The underlying principals were extended to the materials with interactions such as hydrogen bonds.

1.3.2 Type of exfoliation process

However, knowing the energy required to overcome interlayer interaction is only a part of the story. The applied energy into the system is used for two different types of cracking, interlayer cracking, otherwise known as exfoliation, and fragmentation, which leads to a reduction in lateral particle size. Fragmentation has double-faced tactics. On the one hand, it can reduce the lateral size of graphene. This is not desirable for achieving large-area

graphene. On the other hand, it facilitates exfoliation because smaller graphite fakes are easier to exfoliate than larger ones because of smaller collective van der Waals interaction forces between the layers in smaller graphite flakes.

The type and extent of the forces exerted during the exfoliation determine which process will be effective and efficient. Various forms of forces and energy transfers can occur in the system, depending on the process of choice. For example, sonication generates cavitation, micro bubble explosions, and as a result, compressive forces and normal tensile forces work against each other to slip layers over each other. On the other hand, in the high shear exfoliation process, it is the shock waves, random collisions and flow channels that lead to shear forces that help the layer exfoliation and fragmentations.

1.3.3 Environmental impact

Once exfoliated, isolated 2D layers should be stabilised against flocculating to stop going back to their natural bulk states. Stability of the 2D dispersions is typically enforced by introducing dispersing agents, such as surfactant molecules and polymers, to generate new forces such as π–π conjugation, hydrophobic force and Coulomb attraction and matching the surface energy of graphene layers to that of the exfoliation media [27]. The organic solvent is a very commonly used liquid media in exfoliation. However, its hazardous nature hinders widespread application in the industry due to safety concerns (30). Hence, with the aid of surfactant stabilisers, aqueous solutions stand out as a more environmentally friendly option for high-yield exfoliation (30). Surfactants can be divided into several classes according to the head group, and the most popular ones are ionic and non-ionic surfactants (30). According to Guardia et al. (36), because the steric repulsion of non-ionic surfactants is stronger than the ionic electrostatic repulsion, graphene can be better dispersed and stabilised in them, which results in higher graphene dispersion. Nevertheless, surfactants are electrically insulating and almost impossible to remove. This intrinsic nature thus limits the electrical properties of the product and causes a higher cost and further environmental problems (37).

1.3.4 Thermodynamic law of exfoliation

The underlying scientific principle of the energy distribution of graphite/graphene dispersion is similar to **Griffith Theory of Crack propagation**. To keep the new reality in check, a reduction in potential energy from the old state should be greater than or equal to an increase in surface energy due to the creation of a new state. Energy terms pertaining to a graphene dispersion can be defined as the enthalpy of mixing for graphite in the solvent (DH_m), the energy required to separate all molecules (solvent/graphene sheet) to infinity (DH_α) and the energy to bring them back together in the form of a solvent-graphite dispersion (DH_o), but with flakes of different thickness (38). The energy input of the exfoliation process, along with (DH_m), should compensate for the difference between the (DH_α) and (DH_o).

2. Experimental details

2.1 Methodology

Synthesis: Exfoliation of graphite into few layers graphene was achieved through a number of consecutive steps.

(1) Electrochemical treatment resulting in expanded graphite

An electrochemical cell with two electrodes is used to exfoliate a high purity compressed graphite pellets (HQ graphene). The graphite anode and platinum gauge cathode were mounted using copper crocodile clips and immersed completely in the electrolyte, which was 0.5 M ammonium thiosulphate, pH adjusted with alkaline media to 8-9. A voltage of 8V was applied, and allow the graphite was allowed to expand for 1 hour (see figure 4a). Further details on the reaction mechanism can be found in Achee TC et al. (32).

(2) Intercalation by soaking in intercalant solution

Intercalant (2% tetrabutylammonium sulfate) was added to the resultant expanded graphite dispersion (5mg/mL) for a few days. The mixture was subjected to bath sonication for 30 min to get a homogeneous solution. After soaking for five days, the solution was then sprayed (Graco Magnum 262805 X7 HiBoy Cart Airless Paint Sprayer) into a container at a high-pressure of 2000 psi. This cycle was repeated three times. The solution was then subjected to bath sonication (30 min) and centrifugation (10,000 rpm for 30 min). The supernatant (containing the few-layer graphene) was separated for further processing (figure 4b). Further details are described in Nemala S et al.(39).

Characterisation: Several characterisation techniques were utilised to assess the quality of graphene produced.

X-ray diffraction (XRD):

X-ray diffractograms were collected on a Bruker D2 phaser. High purity (99.999%) Ceylon vein graphite was micronized and deposited on an XRD sample holder. Measurements were taken at 22 °C and 2θ between 10° – 70°.

Raman spectroscopy:

The Raman spectroscopy of the exfoliated samples was carried out using Lab Raman, Jobin Vyon spectrometer: model HR800 using Argon laser of wavelength 514.5 nm. The sample preparation was done by spreading the exfoliated aqueous solution uniformly over a glass substrate and then positioning it below the infra-red (IR) lamp for 10 min. A particular area of the sample was then selected and focussed on the laser beam.

Scanning Electron Microscopy (SEM):

SEM images were recorded using an LEO Gemini 1525 FEG SEM using a 30 μm aperture and operated at 5 kV. Aliquots of 10 μL of the electrochemically exfoliated and pressure exfoliated inks were drop casted onto an ozone-treated silicon wafer and dried.

Transmission electron microscopy (TEM):

High resolution transmission electron microscopy (HR-TEM) images were recorded using JOEL JEM 2100 F field emission gun-transmission electron microscope operated at 200 kV. The sample preparation was carried out by ultrasonication of the aqueous solution in water for about an hour. The homogenous dispersion of the sample was then dropped cast onto a carbon lacey grid for about 2 hours before imaging.

X-ray photoelectron spectroscopy (XPS):

XPS data were obtained using an AXIS Supra instrument from Kratos Analytical having Al Kα source (hν = 1486.6 eV) in the range of 1– 1000 eV to investigate the surface chemical composition of the exfoliated graphene sample. The XPS data fitting and analysis was carried out using the software ESCApe.

3. Results & Discussion

High purity (99.999%) Ceylon vein graphite was used to produce graphene in this study. An X-ray diffractogram (figure 5) was used to analyse the crystallinity of the graphite. The common phases of crystalline graphite are 002, 004, 101 and 112 (40). The prominent crystallographic peaks 002 and 004 indicate a graphite structure that has retained its high crystallinity through the manufacturing processing.

The quality of samples was studied using Raman spectroscopy and is compared with graphite shown in figure 6(a) and 6(b) (41). Figure 6(a) shows the Raman spectra of the high pressure exfoliated graphene, which consists of D band, G band and 2D band related to various vibrational modes. The 'G' band comes from in–plane vibrational mode of sp^2 carbon atoms associated with the E_{2g} phonon. The 'D' band associated with the breathing mode of A_{1g} symmetry of sp^2 hybridised carbon rings. This 'D' band corresponds to the defects present in the graphene sheet. The '2D' band arises due to the second-order Raman scattering process, which signals at double the frequency of the 'D' band (42, 43). In natural vein Ceylon graphite, this 2D band is asymmetric; after the exfoliation process, this band looks symmetric and slightly shifted towards the low wavenumber side, the 'G' band's full width at half maxima is higher for exfoliated graphene. These observations confirming the exfoliation of graphite yielded the exfoliation process through the high-pressure exfoliation process. The intensity ratio of D and G bands is evaluated as 0.85 for exfoliated graphene, which is much higher than that of the natural graphite (0.05), which features the exfoliation of graphite. Various parameters of Raman spectra of exfoliated graphene, in comparison with standard graphite (41), are tabulated in table 1.

The Raman spectra clearly showed the difference between the 2D peaks obtained from the two exfoliation routes. The 2D-band of high pressure exfoliated graphene is symmetric in shape, whereas multiple peaks are visible in the 2D-band of electrochemically exfoliated graphene. The low D/G intensity ratio for the high pressure exfoliated sample as compared to the electrochemically exfoliated material is an indication of low defect concentrations in graphene produced. The symmetric shape and the position of the 2D peak reveal that fewer layers of graphene are produced by high pressure exfoliation.

Scanning electron micrographs show that graphene obtained through the pressure exfoliation route achieved higher concentrations (figure 7a) than electrochemical exfoliation (figure 7b). Follow up morphological investigations by the TEM study revealed the presence of graphene sheets, as shown in figure 8 & 9. The electron diffraction spots are labelled using Miller-Bravais indices (hkl). The ratio of identified peak intensities of 0^{th} order and 1^{st} order spots are indicative of single or multilayer graphene depending on the area under the electron beam. The hexagonal lattice of exfoliated graphene can be observed by the selective area electron diffraction (SAED) pattern with (0-110) and (1-210) reflections, as shown in figure 8 (b) & 9 (b). Compared to patterns in 8(b), the

hexagon is more defined in figure 9 (b), indicating that the high-pressure exfoliation further reduced the number of layers in the flakes. The magnified image in figure 9 (c) confirms that the flakes contain only 1 to 2 layers of graphene. The TEM images and spot patterns of the selected area diffraction and HR TEM images of the high pressure exfoliated graphene shown in figure 9 further revealed stacks consisting of 4 and 3 layers, which is in agreement with the Raman spectroscopy analysis. Results indicate that the increase in the energy input and processing time leads to a reduction in the number of graphene layers in the flakes produced and increased fragmentations.

The XPS survey spectra conducted on the high pressure exfoliated graphene sample is shown in figure 10. The spectrum indicated two distinctive peaks arising from carbon (284 eV) and oxygen (533 eV) contributions. The XPS spectrum of graphene did not contain any elements other than carbon and oxygen, indicating the absence of impurities. On comparing the two peaks, it is evident that C 1s is a dominant peak while the intensity of peak related to O 1s is the secondary peak. Having a smaller O1s peak is a proof that oxygen content in the material is fairly low. However, given that the process of high pressure is not expected to introduce any oxygen to the graphene domains and support TEM results, it seems that the feed stock expanded graphite should have some extent of oxygen.

Conclusion:

We have investigated the quality of graphene produced by a novel processing method that uses combined electrochemical exfoliation and follows by high-pressure shear exfoliation in aqueous media using characterisation techniques; Raman spectroscopy & HR-TEM. Our results divulge that graphene sheets' thickness ranges from a monolayer to 5 atomic few layers graphene (FLG), with the averaged thickness being below five layers. The Electrochemical exfoliation process does not introduce noticeable defects or additional oxidation in the graphene sheets, whereas high pressure creates minor defects. The main advantages of this method are its high efficiency and the controlled quality of exfoliated graphene sheets with a high yield of FLG obtained. We explored the impact of type, energy input and mechanisms involved with different exfoliation processes. We attempted to highlight various factors that can influence the choice of the exfoliation process. The authors would like to conclude that the key to upscaling graphene production for industrial scale, either by batch or continuous process, is to understand the various aspects of the liquid exfoliation routes available. Liquid exfoliation can be implemented as a low cost, high-efficient process for future large-scale industrial production.

Funding Statement
S. Bohm is thankful for the Royal Society Industry fellowship at Imperial College London with the project funded via IF150044 with industry sponsor ArcelorMittal Commercial UK Ltd.

Acknowledgements
The authors would like to thank Ceylon Graphite Corp. for providing the highest purity Vein natural Ceylon graphite. IIT Bombay is acknowledged for providing a TEM characterisation facility. All the journals, authors granted permission using figures are also highly appreciated. FT acknowledges funding from EPSRC grants EP/P02534X/2, EP/R511547/1, EP/T005106/1.

References

1. Novoselov KS, Jiang D, Schedin F, Booth TJ, Khotkevich VV, Morozov SV, Geim AK. 2005, Two-dimensional atomic crystals. *Proc. Natl. Acad. Sci. U. S. A.* **102**, 10451–10453. (doi: 10.1073/pnas.0502848102)

2. Geim AK, Novoselov KS. 2009 The rise of graphene. *In Nanoscience and Technology*, pp. 11–19. Co-Published with Macmillan Publishers Ltd, UK. (doi: 10.1142/9789814287005_0002)

3. Shih C-J et al. 2011 Bi- and trilayer graphene solutions. *Nat. Nanotechnol.* **6**, 439–445. (doi: 10.1038/nnano.2011.94)

4. Blake P, Hill EW, Castro Neto AH, Novoselov KS, Jiang D, Yang R, Booth TJ, Geim AK. 2007 Making graphene visible. *Appl. Phys. Lett.* **91**, 063124. (doi: 10.1063/1.2768624)

5. Novoselov KS, Geim AK, Morozov SV, Jiang D, Zhang Y, Dubonos SV, Grigorieva IV, Firsov AA. 2004 Electric field effect in atomically thin carbon films. *Science* **306**, 666–669. (doi: 10.1126/science.1102896)

6. Balandin AA, Ghosh S, Bao W, Calizo I, Teweldebrhan D, Miao F, Lau CN. 2008 Superior thermal conductivity of single-layer graphene. *Nano Lett.* **8**, 902–907. (doi: 10.1021/nl0731872)

7. Choi W, Lahiri I, Seelaboyina R, Kang YS. 2010 Synthesis of graphene and its applications: A review. *Crit. Rev. Solid State Mater. Sci.* **35**, 52–71. (doi: 10.1080/10408430903505036)

8. Wu Z-S, Pei S, Ren W, Tang D, Gao L, Liu B, Li F, Liu C, Cheng H-M. 2009 Field emission of single-layer graphene films prepared by electrophoretic deposition. *Adv. Mater.* **21**, 1756–1760. (doi: 10.1002/adma.200802560)

9. Eda G, Emrah Unalan H, Rupesinghe N, Amaratunga GAJ, Chhowalla M. 2008 Field emission from graphene based composite thin films. *Appl. Phys. Lett.* **93**, 233502. (doi: 10.1063/1.3028339)

10. Shan C, Yang H, Song J, Han D, Ivaska A, Niu L. 2009 Direct electrochemistry of glucose oxidase and biosensing for glucose based on graphene. *Anal. Chem.* **81**, 2378–2382. (doi: 10.1021/ac802193c)

11. Schedin F, Geim AK, Morozov SV, Hill EW, Blake P, Katsnelson MI, Novoselov KS. 2007 Detection of individual gas molecules adsorbed on graphene. *Nat. Mater.* **6**, 652–655. (doi: 10.1038/nmat1967)

12. Kim KS et al. 2009 Large-scale pattern growth of graphene films for stretchable transparent electrodes. *Nature* **457**, 706–710. (doi: 10.1038/nature07719)

13. Novoselov KS, Jiang D, Schedin F, Booth TJ, V KV, V MS. 2005 Two-dimensional atomic crystals. Proc. Natl. Acad. Sci. U. S. A. **102**, 10451-3.

14. Wang D et al. 2009 Self-assembled TiO2-graphene hybrid nanostructures for enhanced Li-ion insertion. ACS Nano **3** 907–914. (doi: 10.1021/nn900150y)

15. Paek SM, Yoo EJ, Honma I. 2009 Enhanced cyclic performance and lithium storage capacity of SnO_2/graphene nanoporous electrodes with three-dimensionally delaminated flexible structure. *Nano Lett.* **9**, 72-75. (doi: 10.1021/nl802484w)

16. Torrisi F, Carey T. 2018 Printing 2D Materials. In Flexible Carbon-based Electronics, pp. 131–205. Weinheim, Germany: Wiley-VCH Verlag GmbH & Co. KGaA.

17. Torrisi F, Carey T. 2018 Graphene, related two-dimensional crystals and hybrid systems for printed and wearable electronics. *Nano Today* **23**, 73–96. (doi: 10.1016/j.nantod.2018.10.009)

18. Lim JY, Mubarak NM, Abdullah EC, Nizamuddin S, Khalid M, Inamuddin. 2018 Recent trends in the synthesis of graphene and graphene oxide based nanomaterials for removal of heavy metals — A review. *J. Ind. Eng. Chem.* **66**, 29-44. (doi:10.1016/j.jiec.2018.05.028)
19. Agudosi ES, Abdullah EC, Numan A, Mubarak NM, Khalid M, Omar N. 2020 A review of the graphene synthesis routes and its applications in electrochemical energy storage. *Crit. Rev. Solid State Mater. Sci.* **45**, 339–377. (doi: 10.1080/10408436.2019.1632793)
20. Bin WJ, Z R, Y H, Xl Y, Pz L, H Z. 2020 A review of graphene synthesis at low temperatures by CVD methods. *New Carbon Mater.* **35**, 193-208. (doi: 10.1016/S1872-5805(20)60484-X)
21. Muñoz R, Gómez-Aleixandre C. 2013 Review of CVD synthesis of graphene: Review of CVD synthesis of graphene. *Chem. Vap. Depos.* **19**, 297–322. (doi: 10.1002/cvde.201300051)
22. Cheng C, Jia P, Xiao L, Geng J. 2019 Tandem chemical modification/mechanical exfoliation of graphite: Scalable synthesis of high-quality, surface-functionalized graphene. *Carbon N. Y.* **145**, 668–676. (doi: 10.1016/j.carbon.2019.01.079)
23. Yi M, Shen Z. 2015 A review on mechanical exfoliation for the scalable production of graphene. *J. Mater. Chem. A Mater. Energy Sustain.* **3**, 11700–11715. (doi: 10.1039/C5TA00252D)
24. Jayasena B, Subbiah S. 2011 A novel mechanical cleavage method for synthesizing few-layer graphenes. *Nanoscale Res. Lett.* 6, **95**, 1-7. (doi: 10.1186/1556-276X-6-95)
25. Chen J, Duan M, Chen G. 2012 Continuous mechanical exfoliation of graphene sheets via three-roll mill. *J. Mater. Chem.* **22**, 19625. (doi: 10.1039/C2JM33740A)
26. Knieke C, Berger A, Voigt M, Taylor RNK, Röhrl J, Peukert W. 2010 Scalable production of graphene sheets by mechanical delamination. *Carbon N. Y.* **48**, 3196–3204. (doi: 10.1016/j.carbon.2010.05.003)
27. Lu J, Yang JX, Wang J, Lim A, Wang S, Loh KP. 2017 Method for producing a layered (semi)conductive material verfahren. *EU patent.* EP 3, 153 605 1.
28. Bonaccorso F, Lombardo A, Hasan T, Sun Z, Colombo L, Ferrari AC. 2012 Production and processing of graphene and 2d *crystals. Mater. Today* (Kidlington) **15**, 564–589. (doi: 10.1016/S1369-7021(13)70014-2)
29. Karagiannidis PG, Hodge SA, Lombardi L, Tomarchio F, Decorde N, Milana S, Goykhman I, Su Y, Mesite SV, Johnstone DN, Leary RK, Midgley PA, Pugno NM, Torrisi F, Ferrari AC. 2017 Microfluidization of graphite and formulation of graphene-based conductive inks. *ACS Nano* **11**, 2742–2755. (doi: 10.1021/acsnano.6b07735)
30. Amiri A, Naraghi M, Ahmadi G, Soleymaniha M, Shanbedi M. 2018 A review on liquid-phase exfoliation for scalable production of pure graphene, wrinkled, crumpled and functionalized graphene and challenges. *Flatchem* **8**, 40–71. (doi: 10.1016/j.flatc.2018.03.004)
31. Marcano DC, V. KD, Berlin JM, Sinitskii A, Sun Z, Slesarev A. 2010 Improved synthesis of graphene oxide. *ACS Nano* ***4***, 4806-4814. (doi: 10.1021/nn1006368)
32. Achee TC, Sun W, Hope JT, Quitzau SG, Sweeney CB, Shah SA, Habib T, Green MJ. 2018 High-yield scalable graphene nanosheet production from compressed graphite using electrochemical exfoliation. *Sci. Rep.* **8**, 14525. (doi: 10.1038/s41598-018-32741-3)
33. Abdelkader AM, Cooper AJ, Dryfe RAW, Kinloch IA. 2015 How to get between the sheets: a review of recent

works on the electrochemical exfoliation of graphene materials from bulk graphite. *Nanoscale* **7**, 6944–6956. (doi: 10.1039/C4NR06942K)

34. Parvez K, Wu Z-S, Li R, Liu X, Graf R, Feng X, Müllen K. 2014 Exfoliation of graphite into graphene in aqueous solutions of inorganic salts. *J. Am. Chem. Soc.* **136**, 6083–6091. (doi: doi.org/10.1021/ja5017156)

35. Jung JH, Park CH, Ihm J. 2018 A rigorous method of calculating exfoliation energies from first principles. *Nano Lett.* **18**, 2759–2765. (doi: 10.1021/acs.nanolett.7b04201)

36. Guardia L, Fernández-Merino MJ, Paredes JI, Solís-Fernández P, Villar-Rodil S, Martínez-Alonso A, Tascón JMD. 2011 High-throughput production of pristine graphene in an aqueous dispersion assisted by non-ionic surfactants. *Carbon N. Y.* **49**, 1653–1662. (doi: 10.1016/j.carbon.2010.12.049)

37. Ricardo KB, Sendecki A, Liu H. 2014 Surfactant-free exfoliation of graphite in aqueous solutions. *Chem. Commun.* **50**, 2751–2754. (doi: 10.1039/C3CC49273G)

38. Hernandez Y, Nicolosi V, Lotya M, Blighe FM, Sun ZY, De S, McGovern IT, Holland B, Byrne M, Gun'Ko YK, Boland JJ, Niraj P, Duesberg G, Krishnamurthy S, Goodhue R, Hutchison J, Scardaci V, Ferrari AC, Coleman JN. 2008 High-yield production of graphene by liquid-phase exfoliation of graphite. *Nat. Nanotechnol.* **3**, 563–568. (doi: 10.1038/nnano.2008.215)

39. Nemala SS, Aneja KS, Bhargava P, Bohm HLM, Mallick S, Bohm S. 2018 Novel high-pressure airless spray exfoliation method for graphene nanoplatelets as a stable counter electrode in DSSC. *Electrochim. Acta* **285**, 86–93. (doi: 10.1016/j.electacta.2018.07.229)

40. Hewathilaka HPTS, Karunarathne N, Wijayasinghe A, Balasooriya NWB, Arof AK. 2017 Performance of developed natural vein graphite as the anode material of rechargeable lithium ion batteries. *Ionics* **23**, 1417–1422. (doi: 10.1007/s11581-016-1953-1)

41. Nemala SS, Kartikay P, Prathapani S, Bohm HLM, Bhargava P, Bohm S, Mallick S. 2017 Liquid phase high shear exfoliated graphene nanoplatelets as counter electrode material for dye-sensitized solar cells. *J. Colloid Interface Sci.* **499**, 9–16. (doi: 10.1016/j.jcis.2017.03.083)

42. Malard LM, Pimenta MA, Dresselhaus G, Dresselhaus MS. 2009 Raman spectroscopy in graphene. *Phys. Rep*. **473**, 51–87. (doi: 10.1016/j.physrep.2009.02.003)

43. Ferrari AC, Basko DM. 2013 Raman spectroscopy as a versatile tool for studying the properties of graphene. *Nat. Nanotechnol.* **8**, 235–246. (doi: 10.1038/nnano.2013.46)

Table 1: Raman spectra parameters of natural and exfoliated graphene.

Sample	D band (cm^{-1})	G band (cm^{-1})	2 D band (cm^{-1})	I_{2D}/I_G	I_D/I_G
Graphite	1350	1576	**2717**	0.52	0.05
Electrochemical exfoliated FLG	1349	1575	**2702**	0.65	0.54
High Pressure exfoliated FLG	1348	1575	**2692**	0.67	0.85

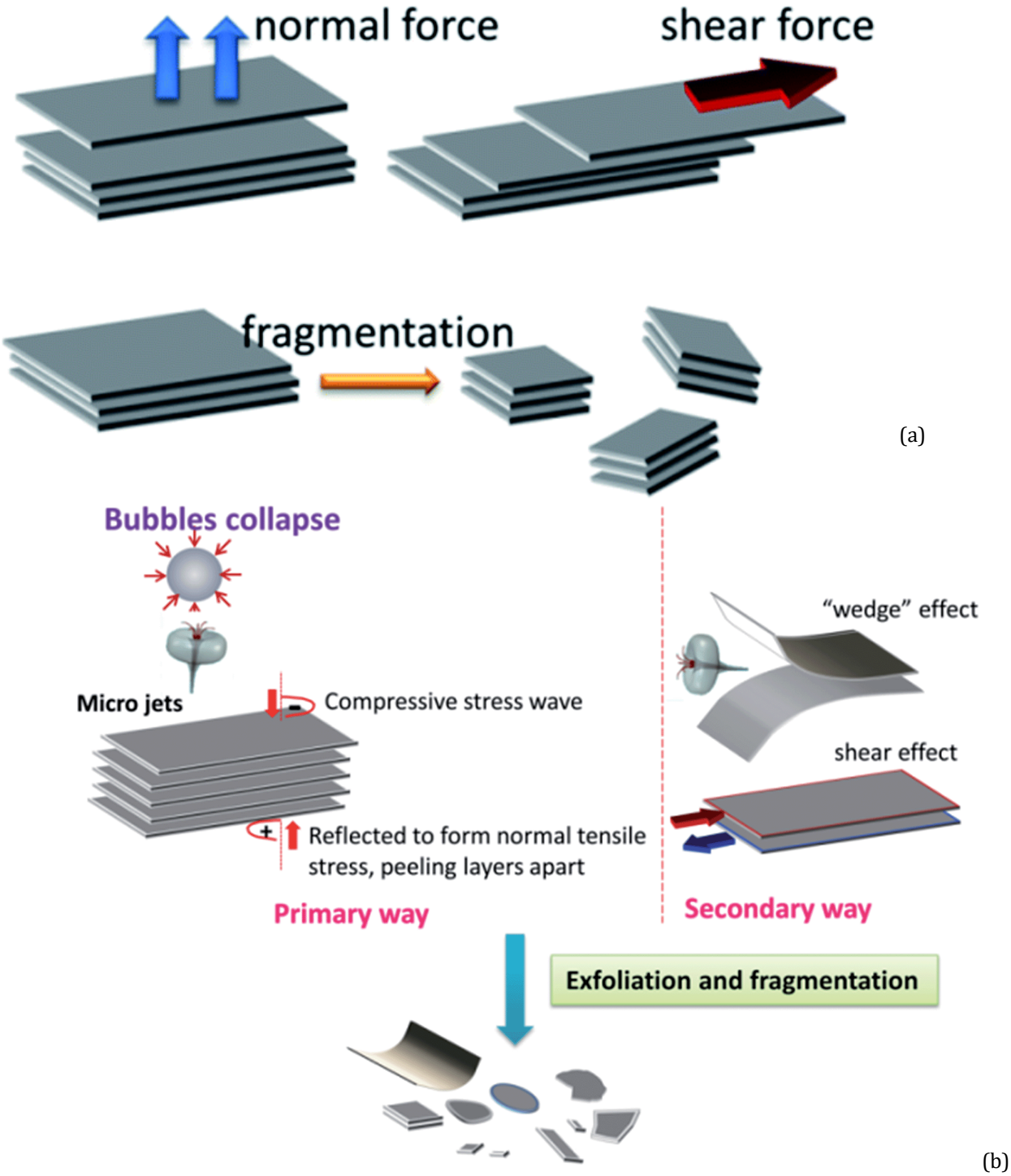

Figure 1. Two types of mechanical force to separate graphite layers(23); (a) The mechanism of liquid-phase exfoliation (b) Mechanism of sonication exfoliation (23).

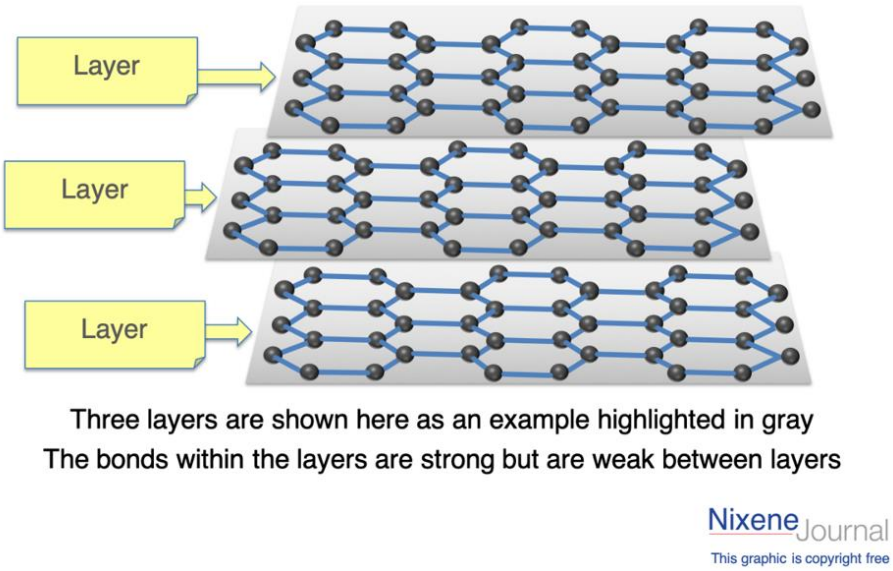

Figure 2. Three layers of graphene connected weakly bonded van der Waals forces.

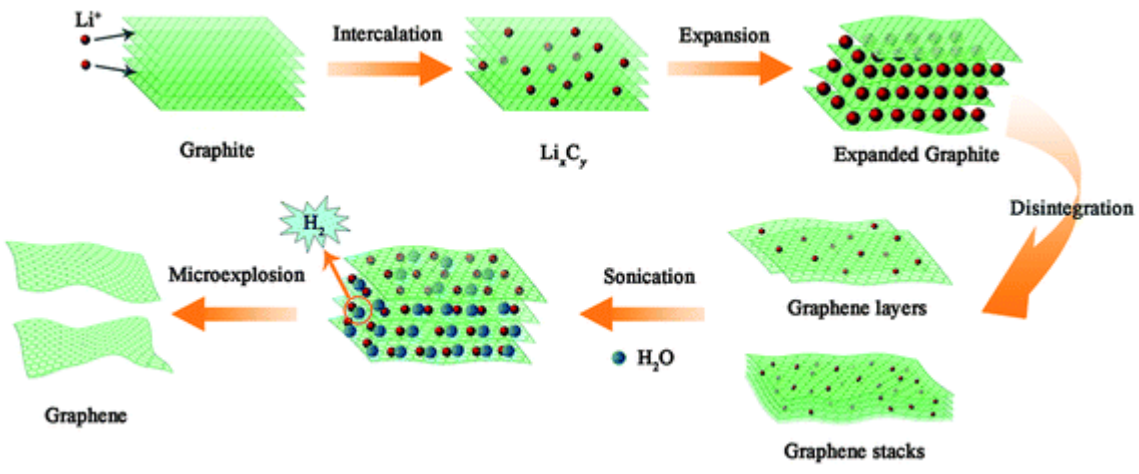

(a)

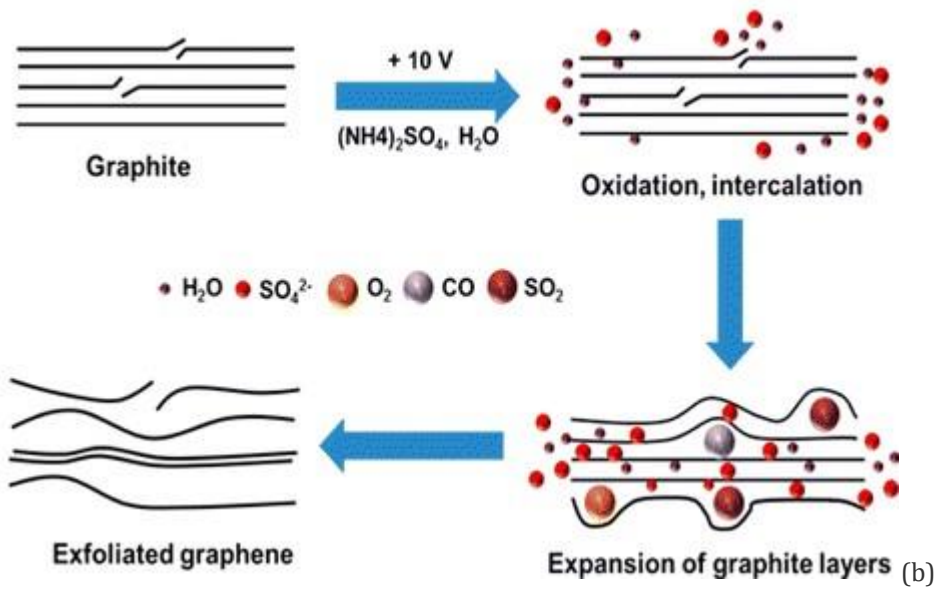

(b)

Figure 3. The mechanism of electrochemical exfoliation in two different electrolytes. (a) Lithium intercalation exfoliation (50); (b) sulfonate salt solution (34).

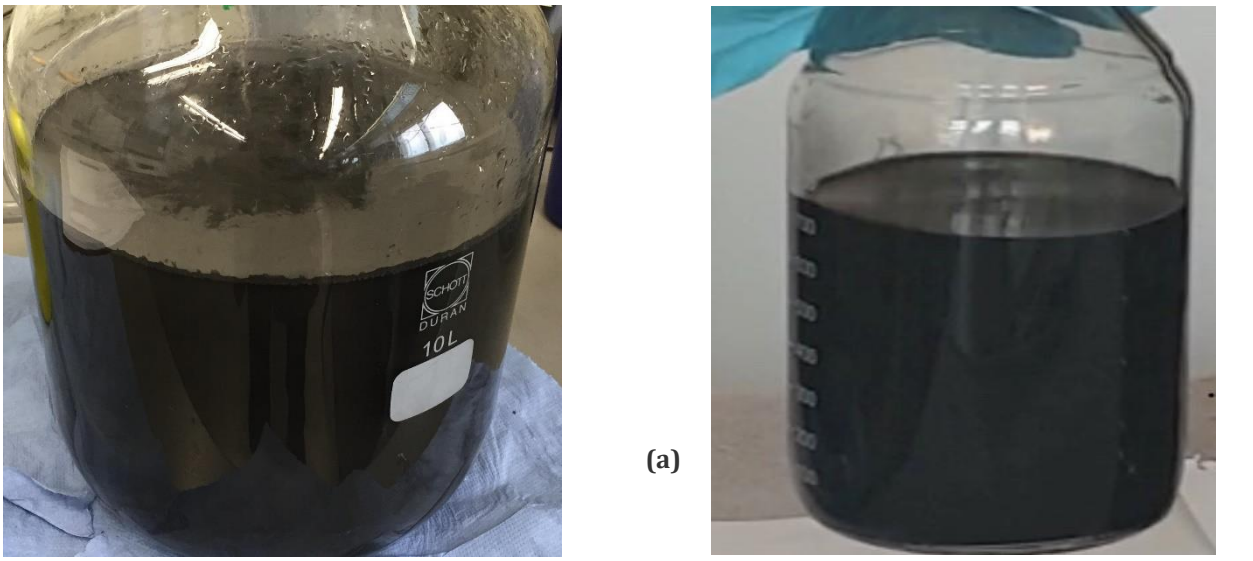

Figure 4. Graphene dispersions (a) electrochemical exfoliation using the high purity materials (Ceylon graphite) compressed as electrode pellets b) high-pressure exfoliation of exfoliated graphene (Ceylon graphite).

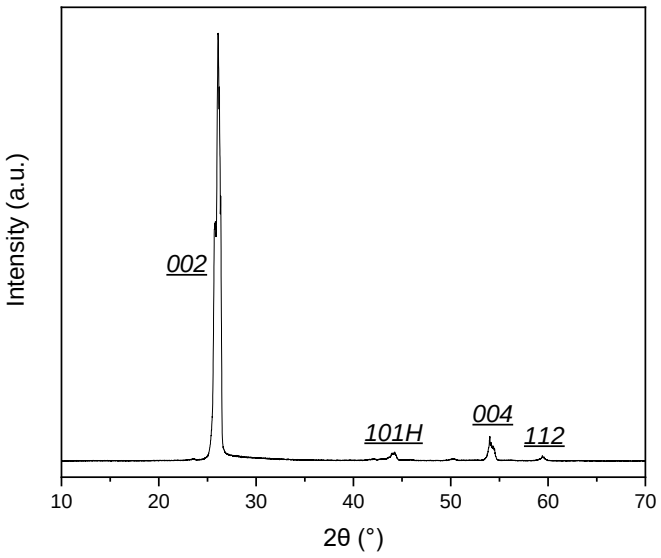

Figure 5: X-ray diffractogram of high purity Ceylon vein graphite (C-99.995%).

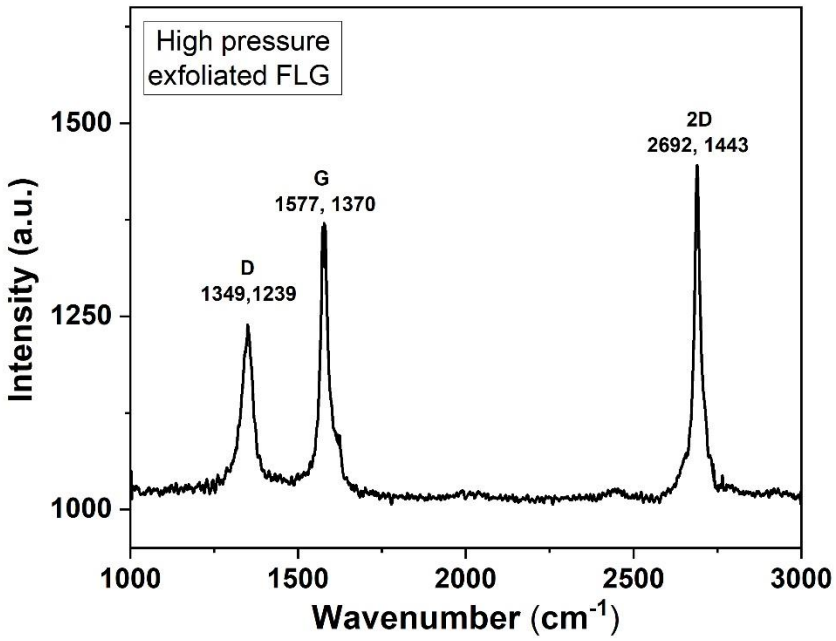

Figure 6a: Raman Spectra of high pressure exfoliated graphene.

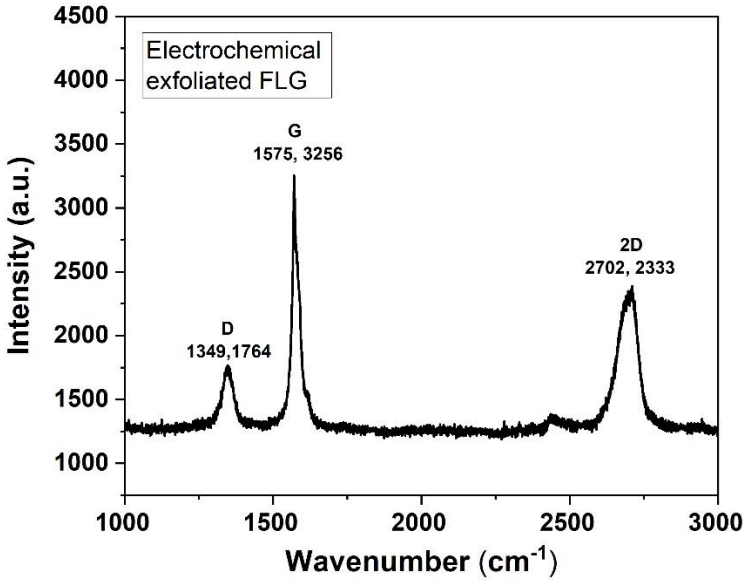

Figure 6b: Raman spectra of electrochemical exfoliated graphene.

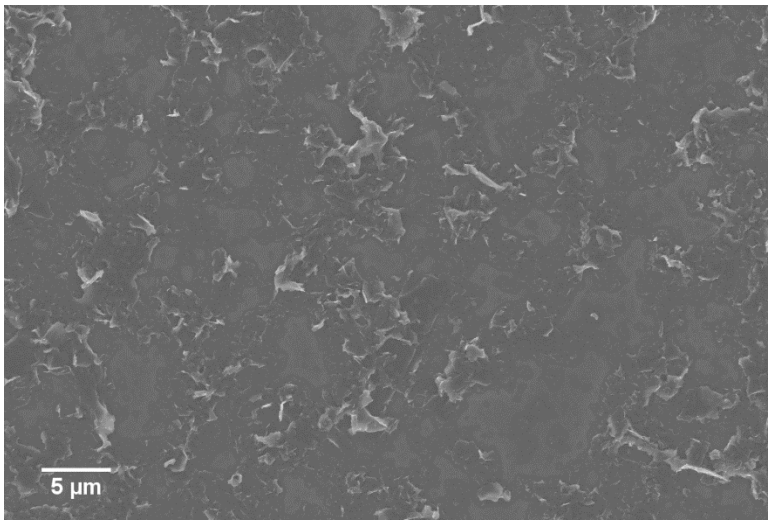

Figure 7a: Scanning electron micrograph of diluted high-pressure exfoliated diluted few layers graphene.

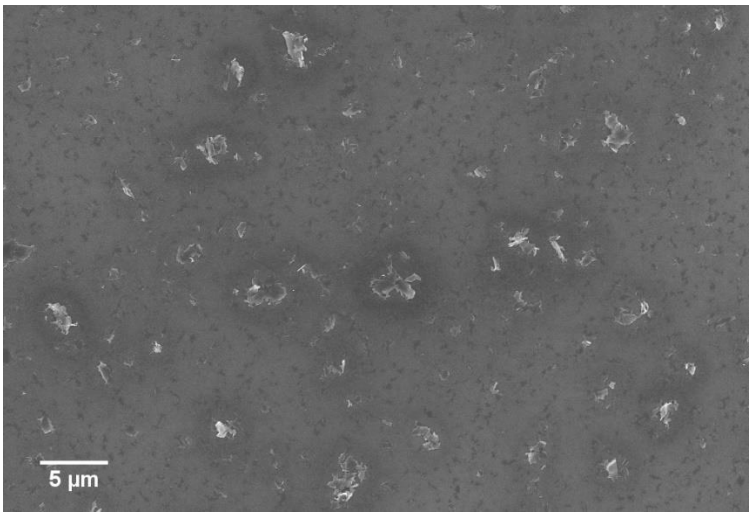

Figure 7b: Scanning electron micrograph of diluted electrochemically exfoliated few layers graphene.

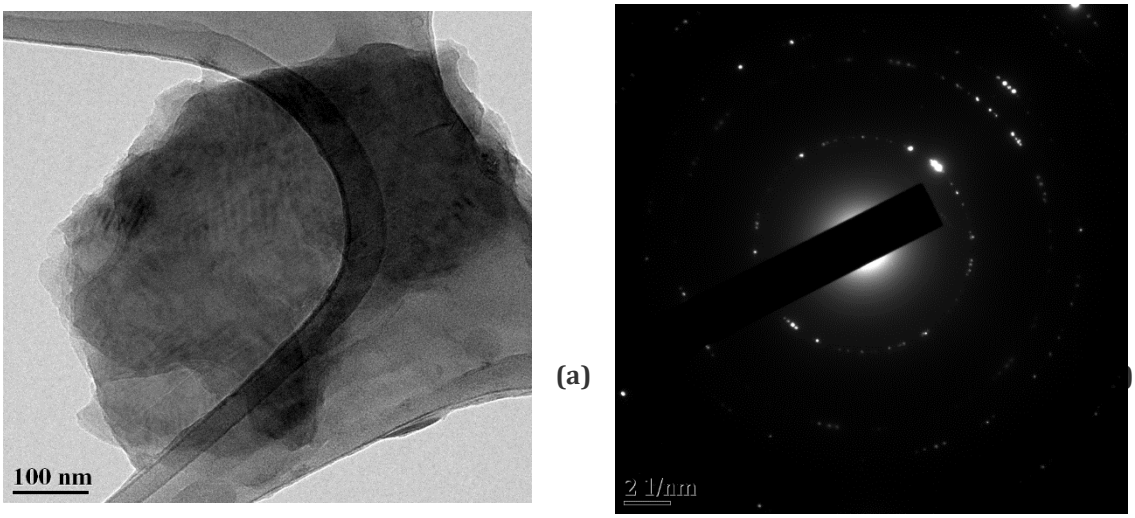

Figure 8 (a): FEG-TEM of electrochemical exfoliated multi-layers graphene**; (b)** SAED pattern of exfoliated multi-layers graphene.

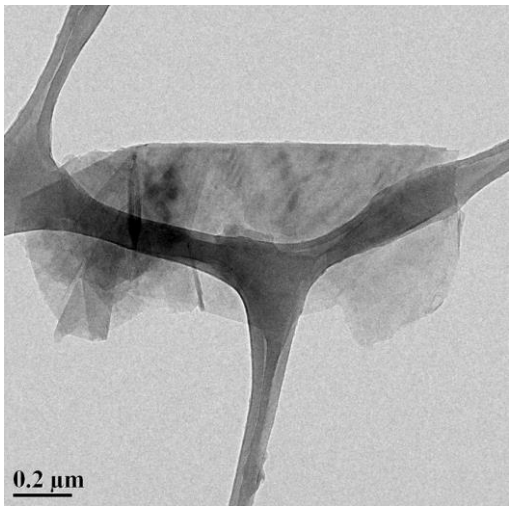

(a)

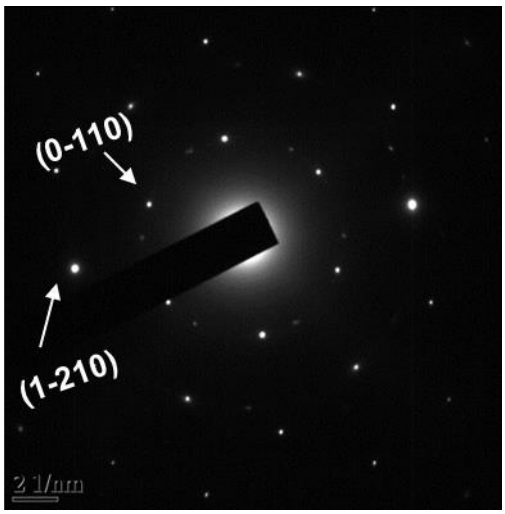

(b)

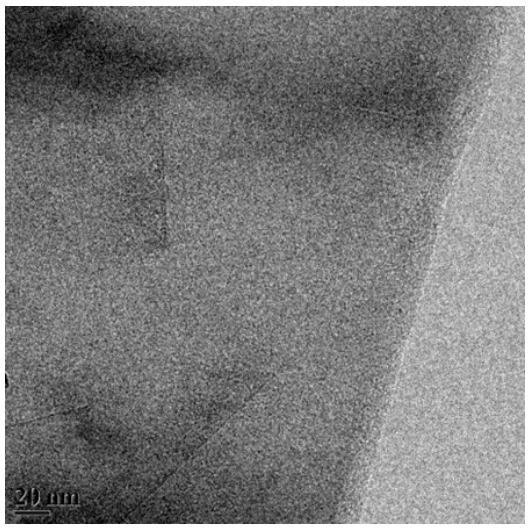

(c)

Figure 9 (a): FEG-TEM of high pressure exfoliated few layers graphene; **(b)** SAED pattern of exfoliated few-layer graphene (c) HR-TEM image of exfoliated graphene showing few layers.

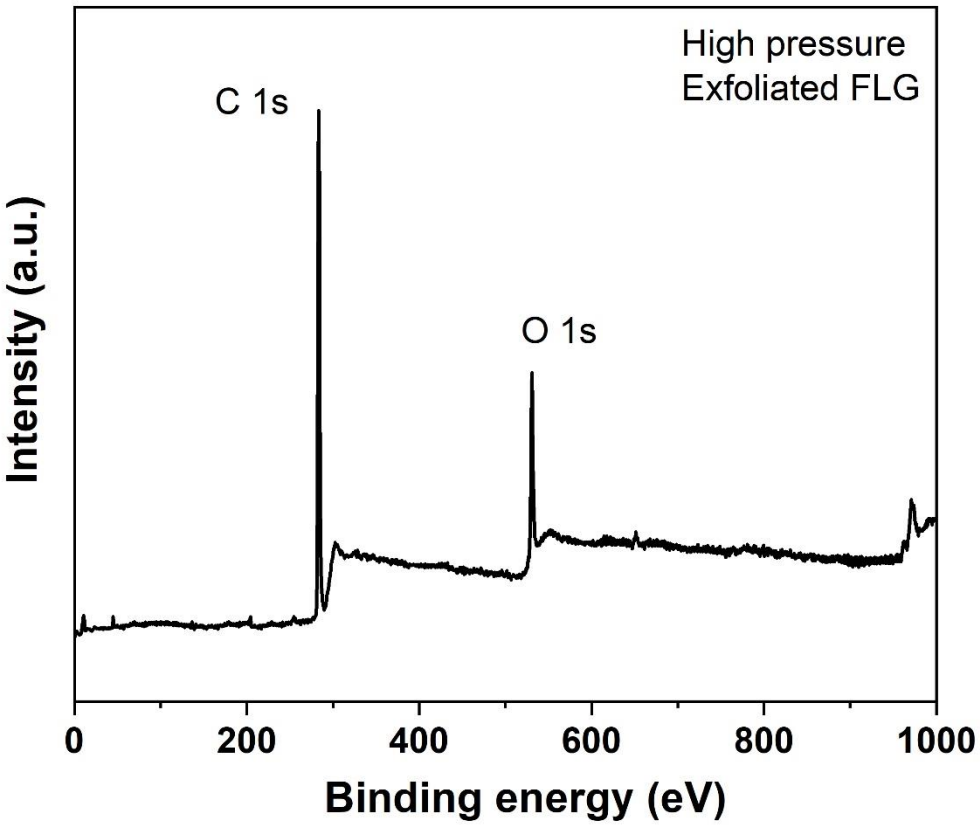

Figure 10: XPS survey spectra of the high pressure exfoliated few-layer graphene.